Transient Control of a Multi Cylinder HCCI Engine During a Drive Cycle

Haraldsson, Göran; Tunestål, Per; Johansson, Bengt; Hyvönen, Jari

Published in:
SAE Special Publications

2005

Leading Our World In Motion

SAE TECHNICAL PAPER SERIES

2005-01-0153

Transient Control of a Multi Cylinder HCCI Engine During a Drive Cycle

Göran Haraldsson, Per Tunestål and Bengt Johansson
Division of Combustion Engines, Lund Institute of Technology

Jari Hyvönen
Fiat-GM Powertrain Sweden

Reprinted From: Homogeneous Charge Compression Ignition (HCCI) Combustion 2005 (SP-1963)

ISBN 0-7680-1636-3

9 780768 016369

2005 SAE World Congress
Detroit, Michigan
April 11-14, 2005

SAE International™

400 Commonwealth Drive, Warrendale, PA 15096-0001 U.S.A. Tel: (724) 776-4841 Fax: (724) 776-5760 Web: www.sae.org

ISSN 0148-7191

Printed in USA

2005-01-0153

Transient Control of a Multi Cylinder HCCI Engine During a Drive Cycle

Göran Haraldsson, Per Tunestål and Bengt Johansson
Division of Combustion Engines, Lund Institute of Technology

Jari Hyvönen
Fiat-GM Powertrain Sweden

ABSTRACT

This study applies a state feedback based Closed-Loop Combustion Control (CLCC) using Fast Thermal Management (FTM) on a multi cylinder Variable Compression Ratio (VCR) engine. At speeds above 1500 rpm is the FTM's bandwidth broadened by using the VCR feature of this engine, according to a predefined map, which is a function of load and engine speed. Below 1500 rpm is the PID based CLCC using VCR applied instead of the FTM while slow cylinder balancing is effectuated by the FTM.

Performance of the two CLCC controllers are evaluated during an European EC2000 drive cycle, while HC, CO and CO2 emissions are measured online by a Fast Response Infrared (FRI) emission equipment. A load and speed map calculated for an 1.6L Opel Astra is used to get reference values for the dynamometer speed and the load control. The drive cycle test is initiated from a hot engine and hence no cold start is included. Commercial RON/MON 92/82 gasoline, which corresponds to US regular, is utilized.

The Linear Quadratic Gaussian (LQG) state feedback controller handles most tasks well, but has some difficulty with retarded combustion phasings, where the controller is outside of its design range. A mean fuel mileage of 6.8 L/100km is achieved, which is an improvement of 13% compared to an equivalent SI simulation using steady state data from the same engine.

INTRODUCTION

The Homogeneous Charge Compression Ignition (HCCI) engine can be understood as a hybrid between the Spark Ignition (SI) and Compression Ignition (CI) engines. In the SI engine, fuel and air are mixed homogeneously before combustion initiation. The charge is then compressed and ignited by a spark plug at the most convenient time for the combustion process. Load control of an SI engine is taken care of by adjusting the amount of mixed air and fuel entering the cylinder. In the CI engine, air is compressed to a higher pressure than in the SI engine, and fuel is injected at high pressure into the hot compressed air and auto-ignition occurs. By adjusting the amount of injected fuel, the load is controlled and hence no throttling is necessary.

HCCI engines use a premixed air and fuel mixture like the SI engine and compress this mixture to auto-ignition like the CI engine. There are various parameters to take into account in order to achieve proper HCCI combustion. Temperature and pressure in the cylinder at the end of the compression stroke, auto ignition properties of the fuel and residual gas fraction all affect the HCCI ignition process. The temperature of the charge has to be higher at the end of the compression phase, compared to the SI engine, in order to cause auto ignition with conventional SI engine fuels.

The first presented results of HCCI engines were performed on 2-stroke engines [1-2]. The primary purpose of using HCCI combustion in 2-stroke engines is to reduce the HC emissions at part load operation, and to decrease fuel consumption by stabilizing the combustion of diluted mixtures. In four-stroke engines, auto ignition can be achieved through a high Compression Ratio (CR), preheating of the inlet air or use of retained residuals [3-11]. In two-strokes, residual gas is always present because of incomplete scavenging, and therefore no preheating is necessary. For 4-stroke engines, HCCI has the potential of combining the desirable features of SI (low NOx and particulates) with the desirable features of CI (high efficiency through low pumping losses and high CR). The low combustion temperature and higher CR with HCCI combustion leads to higher HC and CO emissions than from SI and CI engines [12]. The low exhaust gas temperature is also a problem for the catalyst, since a fairly high temperature compared to HCCI exhaust gas temperature is needed to start the oxidation. Another drawback is the very high heat release rate, which leads to high maximum pressures and noise levels.

To avoid too fast combustion, a diluent must be used. The diluent can be any combination of air, residual gas and Exhaust Gas Recirculation (EGR). In four-strokes, exhaust gas residuals is used both as a diluent to slow down combustion and as bulk to control the temperature of the intake mixture. Since the onset of combustion depends on temperature, pressure, and mixture formation in each cylinder, controlling the combustion process is a challenge. One way to monitor the onset of combustion is to measure the cylinder pressure in each cylinder and calculate the accumulated heat release online. The Crank Angle of 50% heat release (CA50) then serves as a quantitative measure of the combustion phasing [13].

Open-loop combustion phasing using Variable Compression Ratio (VCR) is shown in earlier papers [12,14] to result in a large operating range for HCCI, and CR as high as 21:1 is found effective [16,17], even though higher CR is used in later tests with this engine. Closed-Loop Combustion Control (CLCC) using VCR is shown to have potential to handle step changes in a matter of engine cycles [18]. Single cylinder transient Closed-Loop HCCI control using variable valve timing with quite fast response is shown in [19].

Thermal management is shown by Stockinger et al. [5] during steady state operation. A similar thermal management system is suggested by Yang et al. [20] on a single cylinder HCCI engine. The engine of the present study has VCR and inlet air temperature as a means to phase the combustion. The CLCC using Fast Thermal Management (FTM) adjusts the inlet air temperature by using a source of cold ambient air, and a source of hot, from the exhaust energy, recovery-heated air. CA50 for each cylinder is used as feedback for control, i.e. one CA50 controller per cylinder.

In the present study transient performance of a CLCC using the FTM and VCR are investigated experimentally on a multi cylinder engine using an exhaust heat recovery system [16-18,21-24]. In the current engine configuration, mode transfer between HCCI and SI is possible [24]. Since this article focuses on performance of the CA50 state feedback controller during a drive cycle, no effort is made to implement transition maps in this work and hence no cold start either.

The drive cycle used is called EC2000 or Revised Urban+extra urban or Rev. ECE+EUDC or NEDC. Here the name EC2000 [25] is chosen and it consists of an urban part of 195s, which repeats itself four times in a row, i.e. 780s in total. During the urban part a maximum speed of 50km/h is reached. On top of the urban parts a highway part of 400s is added, where speeds up to 120km/h are run. It results in a drive cycle length of 1180s in total.

EXPERIMENTAL APPARATUS

THE ENGINE

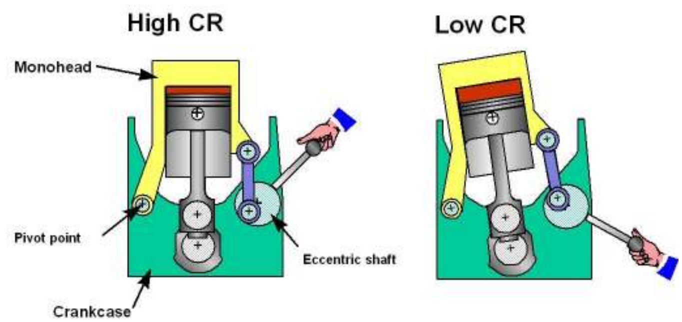

Figure 1 Saab Variable Compression (SVC) engine [26].

The engine used in this study is a five-cylinder 1.6L Saab Variable Compression (SVC) prototype engine. This engine is the basis for a downsized highly boosted SI engine concept [26]. The VCR mechanism of the engine can be seen in Figure 1 and its specifications are given in Table 1.

The geometric CR can be varied continuously between 10:1 and 30:1 by tilting the upper part of the engine up to approximately four degrees by rotating the eccentric shaft. The engine is run naturally aspirated and under conditions corresponding to wide open throttle during the tests presented in this paper. The cylinder pressures are monitored with water-cooled cylinder pressure sensors from Kistler, model 6043A fitted in custom made holes in the cylinder head, one for each cylinder.

Table 1 Geometric specifications of the engine.

Displacement	1598 cm^3 (320 cm^3/cyl)
Number of cylinders	5
Compression Ratio	Adjustable 9–30:1
Bore x Stroke	68mm x 88mm
Exhaust valve open	45°BBDC at 0.15mm lift
Exhaust valve close	7°ATDC at 0.15mm lift
Inlet valve open	7°BTDC at 0.15mm lift
Inlet valve close	34°ABDC at 0.15mm lift
Combustion chamber	Pent roof/four valves DOHC

FAST THERMAL MANAGEMENT SYSTEM

The FTM system consists of a heat exchanger to recover heat from the exhaust, a Three Way Catalyst (TWC) from a Saab 9-5 3.0 V6 and six throttle valves for air mixing. A schematic of the FTM system is shown in Figure 2.

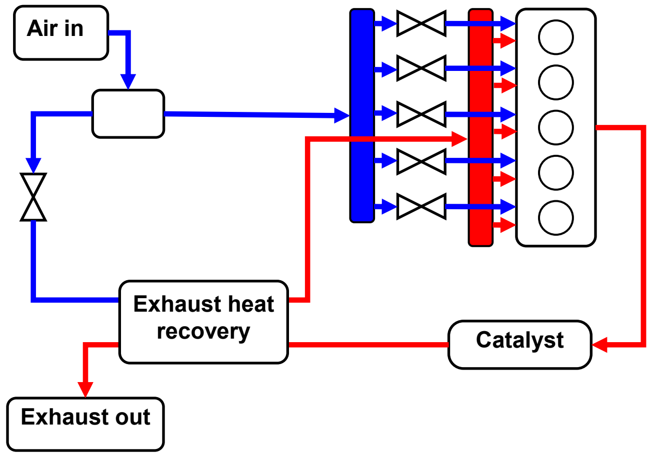

Figure 2 Schematic of the FTM system.

The left throttle controls the amount of hot inlet air and the five throttles in the inlet control the amount of cold ambient air to each cylinder, which means that no additional cylinder balancing, is needed [22]. The engine and its heat recovery system are shown in Figure 3.

Figure 3 SVC engine with cylinder individual FTM system.

SURROUNDING EQUIPMENT

The engine speed is controlled by the dynamometer, which has its own speed controller, where it is possible to set a desired speed from an external system, i.e. our control PC, which is shown in the schematic of the control and measurement system in Figure 4. The dynamometer is a Siemens DC engine of type 1HS5 which can handle powers of up to 325kW, i.e. very large and high inertia compared to this engine. The control equipment for the dynamometer is from Brush Electrical Machines Ltd (and is designed somewhere in the nineteen seventies). The torque is measured with a torque sensor fitted on the shaft between the dynamometer and the engine.

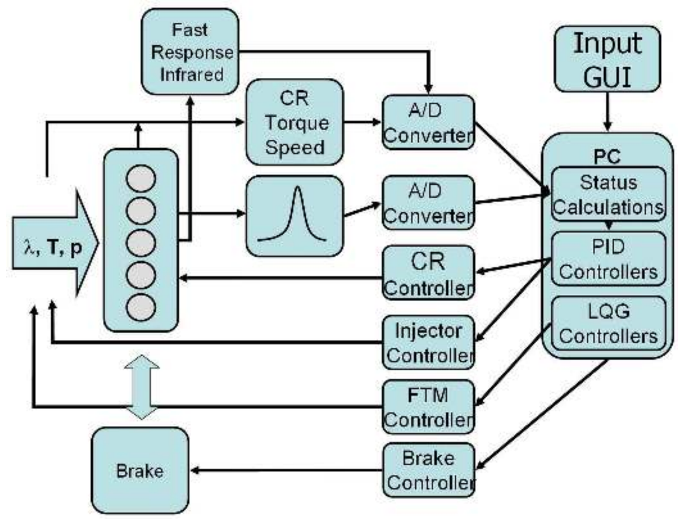

Figure 4 Schematic of the test setup.

Two different emission analyzer systems are used. A Fast Response Infrared (FRI) Horiba MEXA-1300FRI, which measures HC, CO and CO_2 in percent of dry emissions and has a response time ,T_{90}, of 30ms, which is defined as the time to reach 90 % of the final value. The other analyzer system is a Horiba MEXA-8120F, which can measure HC, CO, CO_2, O_2 and NOx, but only the NOx instrument is used on this analyzer. The NOx instrument has T_{90}=1.5s.

Since no complete emission measurement is made with fast instruments, an ETAS LA3 broad band lambda meter, with a cycle time of 2ms, is used. The lambda value from the broad band sensor is calibrated to a complete emission measurement from the MEXA-8120F. In the calculations of emissions NOx is assumed to be zero. This assumption is shown to be reasonably accurate when measuring with the slower NOx instrument, which is sampled at a frequency of approximately 0.33Hz with a HP logger system.

The fuel flow is calculated from injected fuel amount set from the control PC and calibrated by injecting fuel into a container and weighing. At post processing, the fuel flow is double checked by using a fuel balance connected to the slow logger and comparing the fuel flow from both systems. It is found that the slower system shows a 2.6% lower accumulated fuel consumption, but this small difference could also derive from the rather slow update frequency of that system.

CONTROL SYSTEM

HARDWARE

The in-cylinder pressure is sampled with an A/D-converter, DAP 5400a, from Microstar Laboratories capable of sampling 5 samples per CAD and cylinder at the entire speed range of the engine during continuous operation. The other A/D-converter is a multifunction NI6052E card from National Instruments. The NI6052E is run at a sampling rate of one tenth of the DAP rate.

Engine speed, torque, CR, lambda and emissions from the FRI are all sampled by the NI6052E. This card is also used for output to the brake and CR control, while the throttles are controlled by an additional counter board, NI6602 from National Instruments, also connected to the same control PC. With the NI6602, Pulse Width Modulated (PWM) signals are created for all 6 throttles. All three cards are PCI cards installed in a Pentium 4, 2.8GHz hyper threading PC using Windows XP as operating system.

CONTROLLERS

The PID based CLCC using FTM are described in [21]. This system is further developed in [23], where state feedback controllers are designed based on the Linear Quadratic Gaussian (LQG) technique which is a model based approach. The engine model was obtained from system identification by exciting the engine inputs in Figure 5 with Pseudo Random Binary Sequences (PRBS). The engine model is then identified by using subspace methods [27], in this case the n4sid function in Matlab.

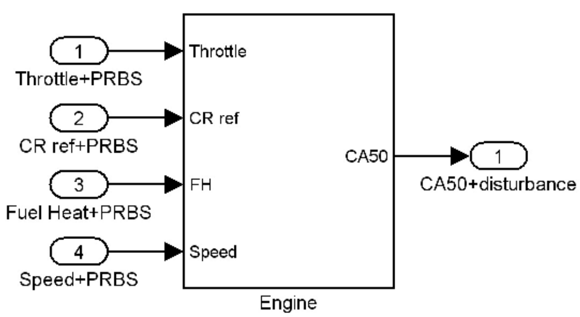

Figure 5 Identification of a black box engine model by adding PRBS signals to disturb the process.

The states, x, for the engine model, are calculated like this:

$$
\begin{aligned}
x_{k+1} &= Ax_k + Bu_k + w_k \\
y_k &= Cx_k + Du_k + v_k
\end{aligned}
\qquad \text{(Eq. 1)}
$$

In Eq. (1), w_k and v_k are white process and measurement noise respectively. y_k is CA50 and u_k is a vector consisting of throttle, CR, fuel heat and engine speed. The A, B, C and D matrices are results of the system identification. From this a state feedback controller is designed, with a structure:

$$
\begin{aligned}
z_{k+1} &= A_c z_k + B_c e_k \\
u_k &= C_c z_k + D_c e_k
\end{aligned}
\qquad \text{(Eq. 2)}
$$

where e_k is the difference between CA50 reference and CA50 at cycle k and u_k is a scalar containing the throttle command. The z-vector contains the controller states. The states in the state feedback controller can be said to know everything worth knowing of the system's earlier history to be able to tell how the system will behave in the future [28]. Note the index c, which shows that it is not the same A, B, C and D as found from the identification in Eq. 1, however those are used to create the new matrices in Eq. 2.

There are actually 2 state feedback controllers for each cylinder. One is used when the mean of CA50 + $CA50_{ref}$ is later than 9 CAD ATDC and the other when it is earlier than 5 CAD ATDC. Between 5 and 9 the controller outputs are weighted together linearly. This solution is chosen since it was difficult to identify the system at retarded CA50s and hence no acceptable model was found for retarded CA50s.

The state feedback controller in Figure 6 uses speed, injected fuel (Fuel Heat), CR_{ref} and CA50 error as input. Output is the throttle control signal, which results in an inlet air temperature change to minimize the controller error, i.e. CA50 error. Previous study showed a difficulty in measuring inlet air temperature during transients and hence no such measurements are made here [21].

Speed, FH and CR_{ref} are only used to enable feed forward action. However due to some imperfection in the identified engine model the speed input is set to a constant value, which improved performance of the controller. This phenomenon could be due to the rather low excitation frequency of speed compared to the other excited variables [23].

During identification of the engine model [23], speeds below 1500 rpm are not included due to large differences in system behavior. This difference can be explained by two effects. The first effect is the Low Temperature Reactions (LTR), which are present with the current fuel at high CR [21]. When LTR are present the need for inlet air heating decreases dramatically. The other effect is the oversized throttle area of the five cylinder-individual throttles, which leads to a negligible effect on inlet air temperature during fast transients from low engine speeds.

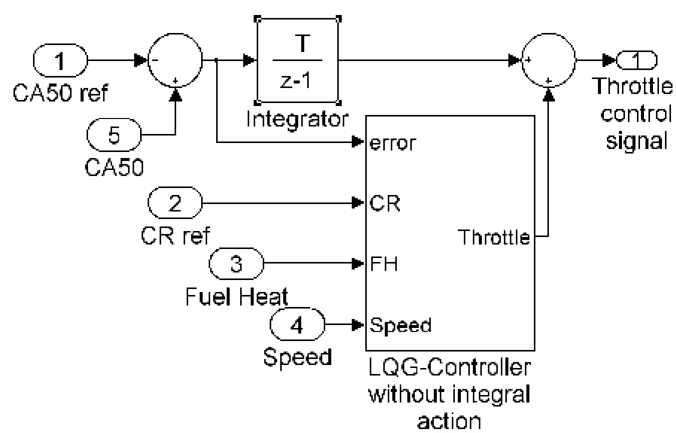

Figure 6 The FTM state feedback controller for CA50 control above 1500 rpm.

A new control strategy is thus applied, with the PID based CLCC using CR at speeds below 1500 rpm, while doing slow cylinder balancing with the cylinder individual throttles. When speed is increased above 1500 rpm the state feedback based CLCC using FTM takes care of CA50 control and CR is slowly changed back to the predefined map in Figure 7. This map deviates some from the ideal CR map used at mean steady state measuring points, which more thoroughly is discussed in the results section.

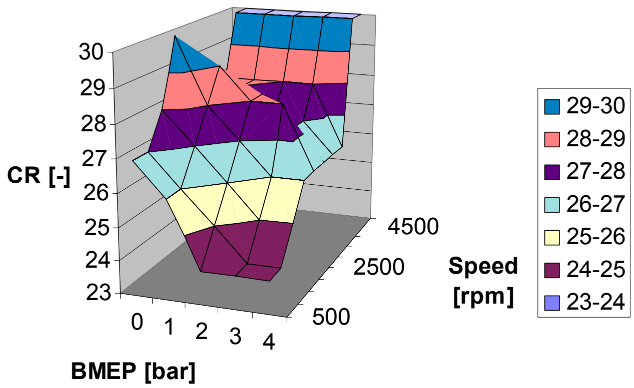

Figure 7 Used CR map at speeds above 1500 rpm.

The PID based CLCC using CR consists of cascade coupled PID controllers where CR reference is set by the combustion phasing controller and the PID based CR controller sets a hydraulic valve, which adjusts the actual CR [18]. The CA50 reference value during the drive cycle is taken from a map optimized for transient operation, which is shown in Figure 8.

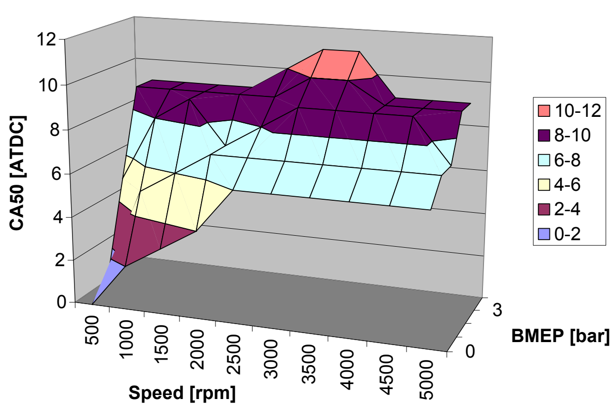

Figure 8 Used CA50 reference map as a function of load and speed.

The load is controlled by a PID controller where BMEP is calculated from the torque measurement and compared to the set point taken from the drive cycle map. Speed is measured by counting clock pulses from the crank encoder. The dynamometer controller receives a reference value from the control PC according to time elapsed in the drive cycle map.

TEST STRATEGY

Two main approaches to cover the EC2000 drive cycle are experimentally tested here. The first approach is to scale the engine size to 3.0L. Load is calculated for a 3.0L engine, with all other variables held constant, e.g. car size and weight. The same scaling factor is used for fuel flow, which also affects the emissions. The scaling approach could be questioned, but the main issue here is the state feedback controller performance. With the scaling of the engine the load range is from -1.1 bar BMEP at deceleration to 4.1 bar BMEP as maximum load. The scaling approach is shown in Figure 9, where the mean steady state maximum load curve as a function of speed is represented by a thick line and the calculated load and speed needed to keep a desired vehicle speed according to the EC2000 drive cycle is represented by circles.

The maximum load is chosen as this engine's maximum load in steady state tests, naturally aspirated, without having too high maximum rate of pressure rise or producing higher NOx emissions than 15 ppm. This happens to coincide with an engine size of 3.0L and hence the reason to scale engine to this size i.e. drive cycle scaled for a 3.0L engine. With a turbocharger higher loads are possible though and it should be possible to cover the entire load range with the 1.6L engine [17].

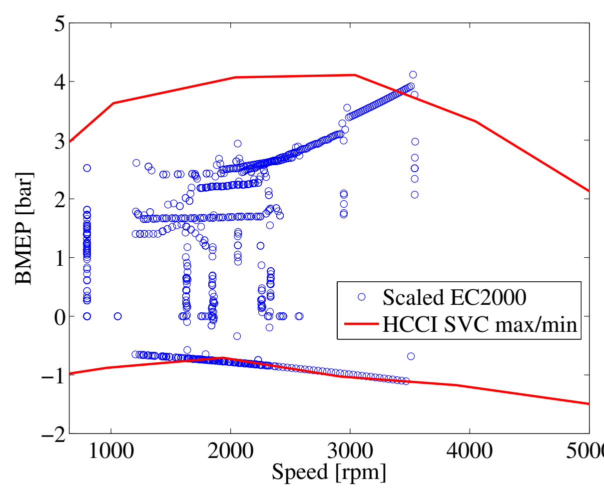

Figure 9 Scaled 3.0L drive cycle points together with maximum and minimum load curve for the HCCI SVC engine as a function of speed.

The second and more realistic approach is quite extensively discussed in the combustion phasing paragraph. It consists of a mix of experimental transient HCCI operation as long as the load is below 3.0 bar BMEP and steady state SI operation above, i.e. no scaling is made here and no actual mode transfer. The load and engine speed for this approach is shown in Figure 10, where the grey represents the SI operating region, the circles represents the drive cycle load as a function of speed and the curve represents the mean steady state HCCI maximum and minimum load as a function of speed. In Figure 10 there is an SI area below the maximum load curve derived from mean steady state data. It would probably be possible to use the maximum load curve as the limit where to switch to SI, but a constant limit proved easier at the time for the test. This is discussed additionally in the discussions paragraph. There exists some drive cycle points below the minimum load curve. This will limit the drivability.

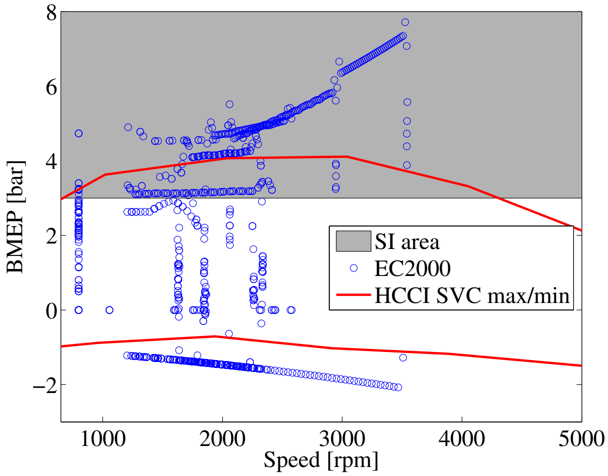

Figure 10 Combined HCCI-SI drive cycle load points as a function of speed

The SI data consists of steady state mean data points as a function of load and speed from which emissions and fuel consumption data is interpolated. The SI data is limited in range between 0 and 8 bar BMEP and 1000 to 3000 rpm while the speed range in the drive cycle is between 800 and 3543 rpm. For the standard 1.6L approach there is a difference in the speed range but since especially the fuel consumption is a rather strong function of load and rater flat in terms of engine speed this should be accurate enough. When simulating the SI drive cycles load below 0 bar is needed, but since the emissions and fuel consumption figures in that area are insignificant the error should be relatively small. Remember that the data below 3 bar only is used for the SI simulations and when interpolating outside the data range the nearest value is chosen and hence no extrapolation is made.

The SI data are taken from SI reference tests in the same test cell on the same SVC engine before it was rebuilt for HCCI operation with its original engine control system, which is optimized for low fuel consumption, however no optimization is made for the emissions in terms of lambda control and flow profile to the TWC. It should be remembered when comparing fuel consumption data that the prototype SI SVC engine already has a comparably low fuel consumption, which is shown in Figure 11. The SVC engine is compared to a scatter band of 3.0L naturally aspirated (NA) engines with comparable torque and power [26]. The same load point in HCCI operation is added in Figure 11.

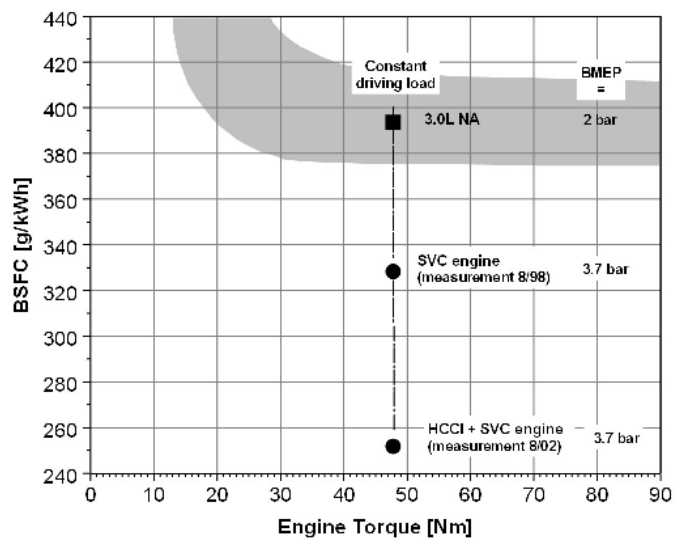

Figure 11 BSFC for the SVC engine in both SI and HCCI configuration compared to 3.0L engines [26].

To be able to compare the fuel consumption and emission data for the two test approaches, simulations with the SI data is made for a 1.6L engine, and a 3.0L engine for the entire load and speed range. In these two tests all data are interpolated from the SI reference data.

An attempt is made to show how much a perfect combustion phasing controller could improve performance compared to the 1.6L combined HCCI-SI approach. The idea is to use steady state SI data as before, but replace the transient HCCI data with mean steady state optimized data, where optimum CA50, CR and inlet air temperature are used.

Note that all data here is experimental with the only difference that some data is mean steady state data used to simulate a drive cycle by interpolation, while the transient data is saved during actual drive cycle tests.

RESULTS

COMBUSTION PHASING

In this section the focus lies in the controller's ability to follow a reference value. The most demanding of the chosen test approaches is the 1.6L HCCI-SI due to the higher mean load. Higher loads results in open-loop instability of the HCCI combustion shown by Olsson et al. [15], which has to be taken care of by the controller. A retarded CA50 is needed to limit the maximum rate of pressure rise, peak cylinder pressure and NOx emissions at high loads. When retarding CA50 the in-cylinder temperature decrease as the auto ignition sets off due to an already expanding charge. This means that it is very sensitive to variations, which lead to cycle-to-cycle variations in CA50 increase.

The engine speeds in the drive cycle map range between idle at 800 and a maximum speed of 3543 rpm. The oversized dynamometer and its rather primitive controller's ability to follow the reference from the speed map are shown in Figure 12. The thin line represents the set value from the map and the thick line represents the actual engine speed, while the grey area represents the simulated SI operation, i.e. load above 3.0 bar BMEP.

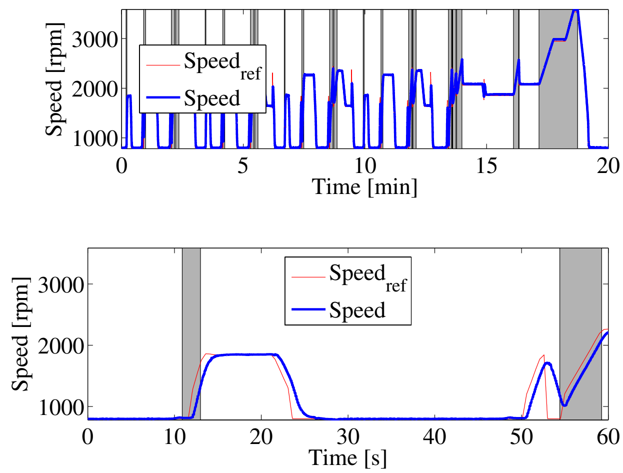

Figure 12 Engine speed during drive cycle test with SI area in grey.

The RMS and mean –deviation are given in Table 2, which gives an indication of how good the dynamometer and engine system follows the reference value. The RMS deviation of 130.2 rpm is acceptable with the dynamometer used here and the mean deviation of 39.3 rpm shows that there is small offset from the desired set value. The lower plot is a close up of the first 60s from the upper plot. With a maximum load of 3 bar BMEP, HCCI operation cover as much as 81% of the entire drive cycle time.

Table 2 RMS and mean deviation from reference values during drive cycle test for scaled 3.0L and 1.6L for the HCCI operation.

	RMS deviation		Mean deviation	
Test case	3.0L	1.6L	3.0L	1.6L
Speed [rpm]	120.5	130.2	19.1	39.3
BMEP [bar]	0.3	0.4	0	0.1
CR [-]	0.2	1.1	0	0.2
CA50 Cyl1 [CAD]	2.6	6.7	0.4	2.2
CA50 Cyl2 [CAD]	2.5	6.6	0.2	2.1
CA50 Cyl3 [CAD]	2.6	6.5	0.3	1.9
CA50 Cyl4 [CAD]	2.5	6.4	0.7	2.2
CA50 Cyl5 [CAD]	2.7	6.7	0.1	1.9

The other variable except time taken from the drive cycle map is the desired load given in bar BMEP. The lower plot in Figure 13 is a close up of the first 60s from the upper plot. The tick line represents the measured BMEP, while the thin line, which is truncated at 3 bar BMEP, represents the set value to the load controller given by the drive cycle map, EC2000 represented by the thin line above 3 bar BMEP. The deviation between the EC2000 line and the $BMEP_{ref}$ line together with a grey background shows the SI parts. During imagined SI operation the load is kept constant at 3 bar BMEP shown in Figure 13. The RMS deviation is 0.4 bar, which is a result of the oscillations around the set value, which is proven by a mean deviation of merely 0.1 bar.

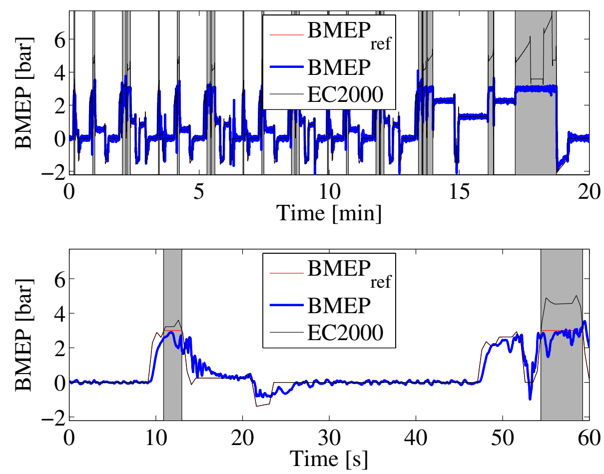

Figure 13 BMEP during drive cycle test with SI area in grey.

The combustion phasing, which is the main goal to control on an HCCI engine, to be able to run at a wide load and speed range, is shown in Figure 14. The thin line represents reference value taken from the predefined map in Figure 8, while the thick line represents the mean CA50 for all five cylinders. The used reference values of CA50 for this load and speed range are between 1.2 and 10.0 CAD ATDC. The advanced combustion phasing is used for low load and speed while the retarded is used for high load and speed.

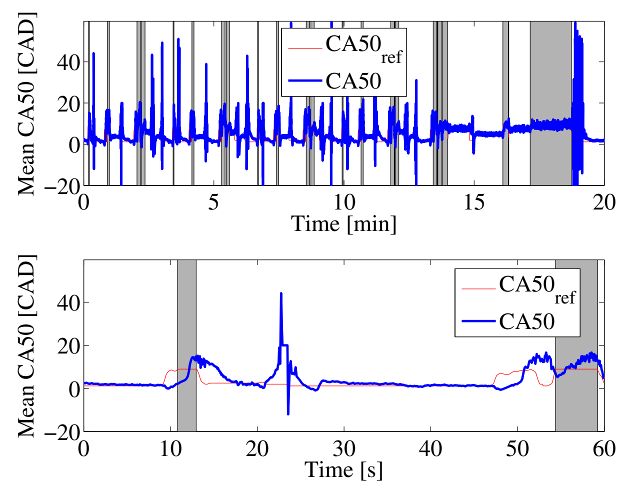

Figure 14 CA50 reference from map and resulting mean CA50 of all cylinders during the drive cycle with SI area in grey.

It can be seen in the lower plot in Figure 14 that there are some deviations from the set value and even total misfires. A reason for advanced CA50 is shown 10s from start where an increase in load results in a retard in CA50 reference according to Figure 8, where it can be noticed that CA50 reference is a strong function of load. The large advance results in the controller error increase. It is however reduced below 5 CAD in approximately 2s.

The retarded CA50s can be explained by looking at Figure 15, where the cold throttle reference value for each cylinder are shown in the upper plot, CR and CR_{ref} in the second plot, CA50 for all cylinders together with $CA50_{ref}$ in the third plot and corresponding load and speed in the two following plots. The vertical lines show the approximate break points where CLCC controllers change between FTM and CR, i.e. if engine speed is above or below 1500 rpm.

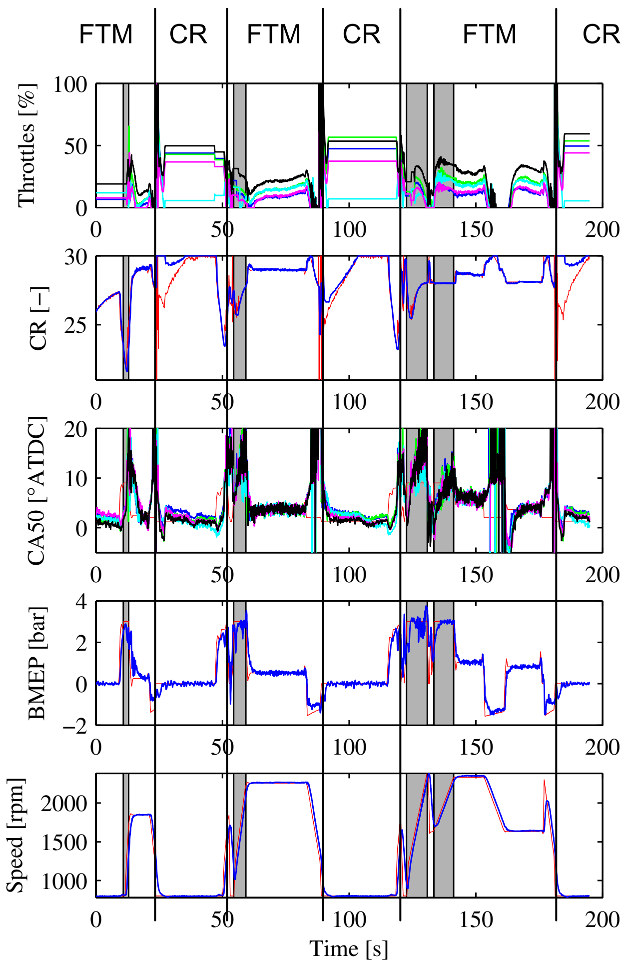

Figure 15 Actuator positions for all five cylinders where the approximate usage of CLCC controller is marked by vertical lines for 200s of the drive cycle with the SI areas marked in grey.

There are mainly two reasons for retarded combustion phasing. The first occurs when the speed is decreased and negative load is applied, which the control program defines as misfire [13], i.e. very retarded CA50 where the CLCC using FTM tries to compensate this, which will result in some smaller oscillations on the throttles, but only with an amplitude of 5 to 10% opening. When the CLCC using CR takes care of CA50 control the CLCC using FTM is turned off and the throttles only perform slow cylinder balancing. At this time the throttles start to oscillate between 0 to 100% opening, which result in some disturbance to the CLCC using CR and on CA50. The phenomenon of the oscillating cylinder balancing throttles are unfortunately due to a minor bug in the control program, which creates these heavy oscillations every time the simple throttle cylinder balancing is applied, i.e. every time the CLCC using CR is turned on.

It should be noted that the cylinder balancing does work as intended in 2s or approximately 20 engine cycles. One typical example is shown at the first vertical line to the left in Figure 15, where CLCC using CR is turned on and the oscillations on the throttles cause the CR_{ref} to drop down to 20:1. However the PID based cascaded coupled CR controller does not change CR as fast as the PID based CLCC changes CR_{ref} and hence it does not automatically result in any more misfires.

The other reason for retarded CA50 is speed and load increase, which results in retarded $CA50_{ref}$ and with the limited performance of the CLCC using FTM at retarded CA50s this results in some overshoot and in the worst case some misfire. Though a faster controller at retarded combustion phasings should be able to correct this.

There seems to be a large number of misfires, i.e. CA50 larger than 20 CAD ATDC, in Figure 14, but if looking at the total number of misfires according to the control program and compare them to the number misfires for load above 0 bar BMEP. The amount of misfires above zero load is 407, which only is 11% of the total number of misfires and 0.5% of the total elapsed engine cycles during the drive cycle.

The large difference in cold throttle opening when applying CLCC using CR in Figure 15 is more an indication of how much less the throttle position affects the air flow during low engine speed than the actual cylinder-to-cylinder variations, which are seen when applying the CLCC using FTM. It shows that it is possible to do cylinder balancing using the FTM [22], but a much larger bandwidth is used at low engine speeds just to balance the cylinders and then there is little bandwidth left to use for other disturbances.

Figure 16 shows a Bode plot of the transfer function from CA50 reference value to measured CA50 for the scaled 3.0L test. The reason to use the scaled is that there are substantially less misfires present due to higher minimum load, but also more advanced $CA50_{ref}$ as a result of the lower maximum load, i.e. the load range is smaller. As discussed before a higher minimum load will result in less misfires found by the control program and the lower maximum load results in less need to retard CA50.

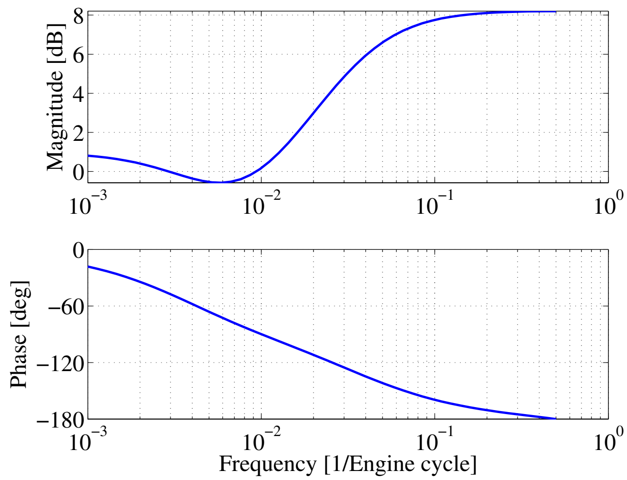

Figure 16 Bode plot of transfer function from CA50 reference to CA50 for the scaled 3.0L test.

This transfer function is derived from the drive cycle data by identifying a single input single output model with CA50 reference as input and CA50 as output. Not that the transfer function includes both CLCC controllers. The static gain is close to unity with a slight negative phase shift which means that the response to reference value changes with low bandwidth is accurate. The Highest frequencies in the reference signal are however amplified and phase shifted. One result of this can be seen in Figure 14 where positive and negative step changes in the CA50 reference result in large overshooting of the measured CA50 and a rather slow response of 2-3s.

FUEL ECONOMY

It is clear from the fuel consumption in Figure 17 that the approach to cover the entire drive cycle by scaling the engine to 3.0L is not a good idea with this engine. One reason is the poor mechanical efficiency of e.g. 62% at 2000 rpm and 2 bar BMEP of this engine [17]. This means that the friction losses severely influence the fuel economy when running the urban parts of the drive cycle where BMEP is very low.

The other reason is the actual scaling which results in decreased load for the same drive cycle load point and hence an increases in the Brake Specific Fuel Consumption (BSFC). The BSFC for mean steady state HCCI data are shown for the scaled 3.0L engine in Figure 18, while mean steady state SI and HCCI data are combined for the standard 1.6L HCCI-SI in Figure 19. Below 1 bar BMEP BSFC increase to infinity at 0 bar BMEP and hence is not plotted below 1 bar BMEP. Each square represents one point in the drive cycle map with a time of 0.5s between. This means that the density of the squares is proportional to the time spent at that specific load and speed and hence BSFC.

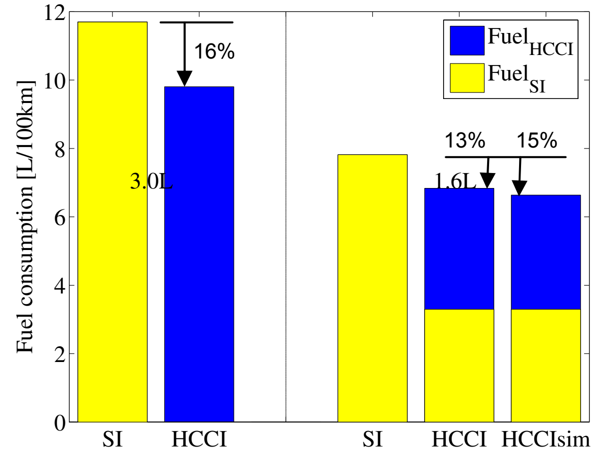

Figure 17 Fuel consumption given in L/100km for both the scaled 3.0L engine and the 1.6L.

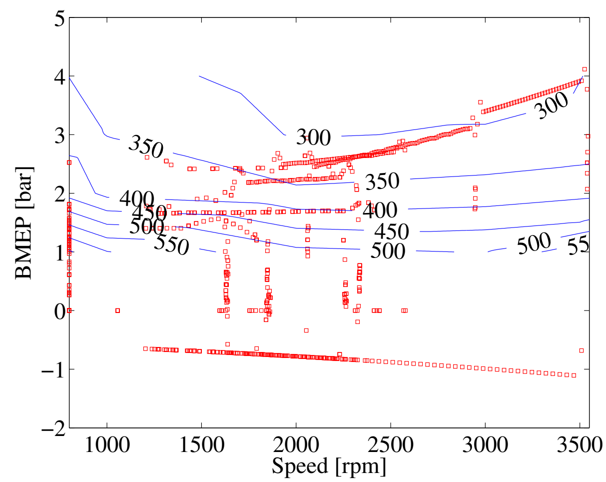

Figure 18 Iso-lines of BSFC for the scaled engine as a function of speed and load together with squares representing the drive cycle points.

The best approach is to run the engine at higher loads to minimize the influence of friction losses, hence no scaling should be done. The gain in running in HCCI mode the entire drive cycle, i.e. scale to 3.0L, is 16% compared to the 3.0L SI simulation. When running in combined HCCI-SI operation a gain of 13% is accomplished compared to the 1.6L SI simulation from steady state mean SI data. The gain by having a perfect CLCC controller for this engine is quantified by the difference between the combined 1.6L transient HCCI-SI and the simulated HCCIsim-SI, which is merely 3%.

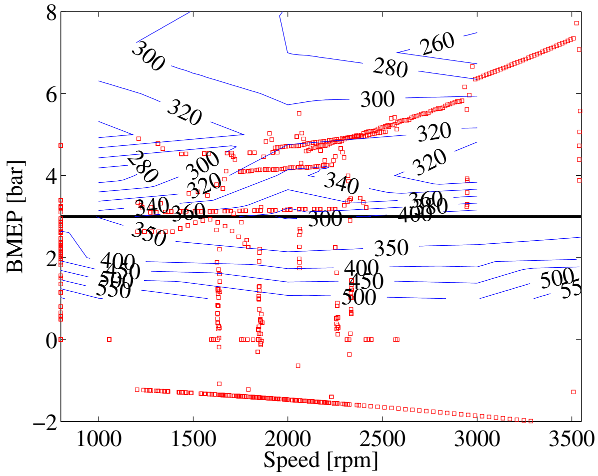

Figure 19 Iso-lines of BSFC for HCCI below the 3 bar line and SI above 3 bar line as a function of speed and load together with squares representing the drive cycle points.

EMISSIONS

A very important issue is to use optimized maps and be able to follow them. If for example CA50 is excessively advanced at high loads NOx emissions will increase, while too retarded CA50 at low loads will result in excessive CO and HC emissions. The emission limits for the Euro IV legislation are given in Table 3. If not using maps for CA50 a goal could be to use as advanced CA50 as possible to minimize HC and CO emissions, but set constraints on maximum allowed rate of pressure rise [29].

Table 3 Legislated Euro IV emission limits for 2006 [25].

	HC [g/km]	CO [g/km]	NOx [g/km]	HC+NOx [g/km]	PM [g/km]
Euro IV Gasoline	0.1	1.0	0.08	-	-
Euro IV Diesel	-	0.50	0.25	0.30	0.025

The accumulated engine out emissions as function of time for the 1.6L combined HCCI-SI are shown in Figure 20, where HC is represented by a dashed dotted line, CO is represented by a dashed line and NOx is represented by a dotted line. It is clear that NOx is almost only accumulated during SI operation while CO accumulation rate decrease during SI operation. It should be noted that the SI SVC engine's emissions are fairly high compared to other comparable SI engines, but as mentioned before the SI engine control system is never optimized for low emissions, i.e. the lambda control and the flow field to the TWC. The emissions after catalyst are calculated both for HCCI and SI operation with a conversion efficiency of approximately 95% for HC and 99% for CO as a function of engine speed [17].

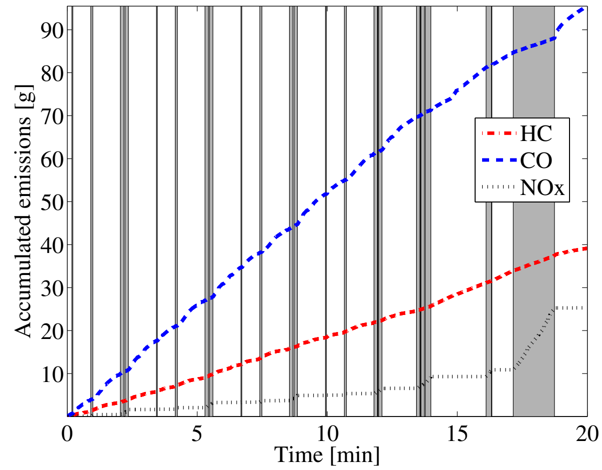

Figure 20 Accumulated engine out emissions for the 1.6L combined HCCI-SI engine during the drive cycle test.

The NOx emissions are engine out emissions, i.e. no reduction of NOx for HCCI, but for SI a conversion efficiency of 99% is used. Differences in conversion efficiency during mode transfer are not accounted for. The accumulated emissions after catalyst for the 1.6L combined HCCI-SI engine are shown in Figure 21 together with the limits for HC and NOx, while the CO limit is much higher and hence not shown.

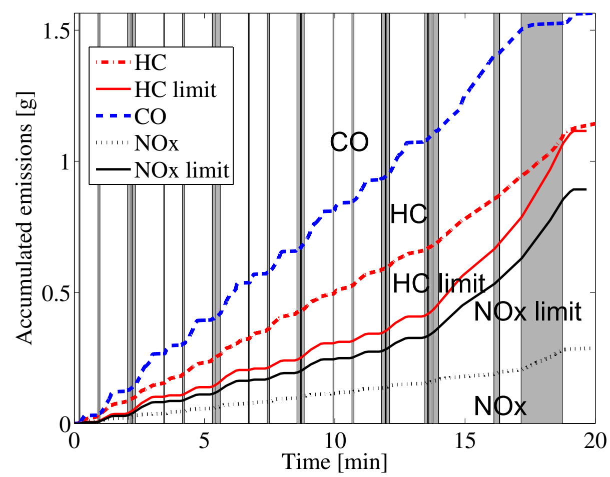

Figure 21 Accumulated emissions after catalyst for the 1.6L combined HCCI-SI engine during the drive cycle test.

Note that it is the final values in Figure 20 and Figure 21 that should be divided by the driving distance, which is 11.007 km, in order to compare the values to the limits in Table 3. The CO_2 emissions are proportional to the fuel consumption and for the transient 1.6L HCCI the CO_2 emissions are 168g/km while the ideal HCCIsim at maximum load reach 160g/km. This is still above the CAFE limit of 140g/km [30]. Additional discussion about the emissions is found in the discussions paragraph.

In Figure 22 to Figure 27 the emissions are given in g/km both engine out, Figure 22 to Figure 24 and after the catalyst, Figure 25 to Figure 27. The contributions of the two operating modes are shown as different parts of the total bars. Those bars labeled with only SI are the simulated SI from mean steady state SI data, while the 3.0L HCCI consists of transient HCCI during an actual drive cycle test. The two labeled 1.6L HCCI consists of both HCCI and SI, while the one labeled HCCIsim consists of mean steady state data for both HCCI and SI, and the bar labeled HCCI consists of transient HCCI data during an actual drive cycle together with mean steady state SI data.

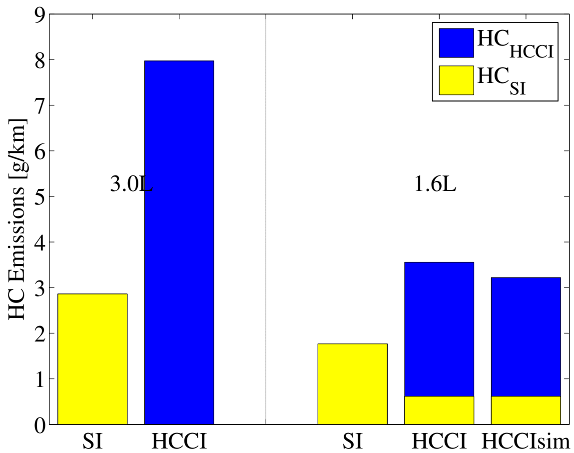

Figure 22 Engine out HC emissions for all five test cases.

The highest engine out emissions of HC and CO are obtained for the scaled 3.0L engine, shown in the left part of these figures. This is due to the scaling, which results in very low load and combustion temperature during the major part of the drive cycle, which result in low combustion efficiency.

The lowest HC emissions are achieved for the 1.6L SI. There are two major effects which counteracts each other. For the 1.6L the higher mean load results in more HC into the crevices, which would result in higher HC emissions for the 1.6L SI, but the scaling effect for the 3.0L engine is more dominating and hence higher HC emissions for the 3.0L engine. The HCCIsim with its “ideal” HCCI shows slightly less HC emissions than the transient 1.6L HCCI and this can be explained by some actual misfires during transients, which are not present in the steady state HCCI data.

The CO engine out emissions in Figure 23 shows very much the same trends as the HC emissions in Figure 22. Here on the other hand there is a larger difference between transient 1.6L HCCI and HCCIsim. With ideal HCCI there is no need to have a lot of control authority of the FTM, i.e. increased bandwidth by adjusting CR. This results in a lower CR used in the ideal HCCI case, which results in lower CO emissions [12]. Even though the CO emissions of the SI SVC engine are relatively high, they are small when compared to the HCCI SVC engine. It should be noted though that the maximum CR is increased from 14 for the SI SVC to 30 for the HCCI SVC engine.

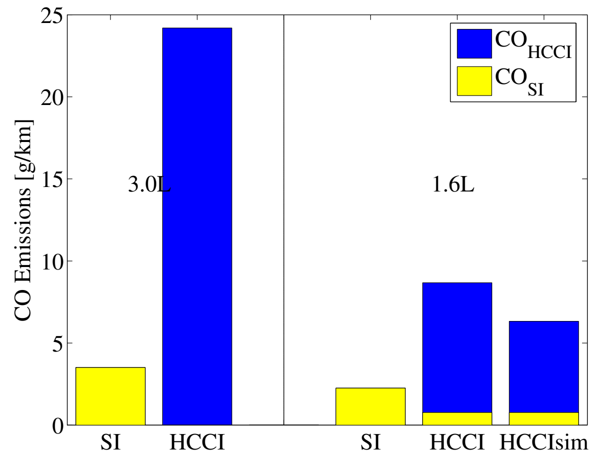

Figure 23 Engine out CO emissions for all five test cases.

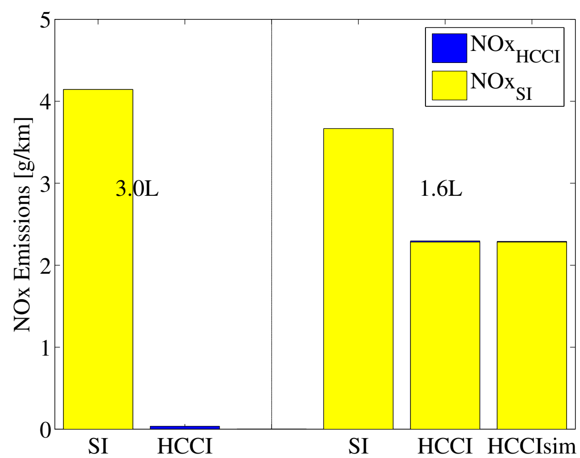

Figure 24 Engine out NOx emissions for all five test cases.

Almost all NOx derive, as expected, from the very much hotter combustion process of the SI SVC engine. Figure 24 shows that it is very advantageous to run in HCCI operation as much as possible if low NOx emissions are desirable. Note that for the transient 1.6L HCCI it is SI combustion during 19% of the time, but the SI combustion produce 99% of the total NOx.

In Figure 25 the Euro IV gasoline limit of HC is plotted on top of the bars. The transient 1.6L HCCI is 3.8% above the limit while the ideal HCCIsim is 6.3% below the limit. It should be noted though, that no cold start is made here and almost all HC during a drive cycle derive from the cold start until the catalyst has light-off [31]. A possible solution could be to use an HC trap [32].

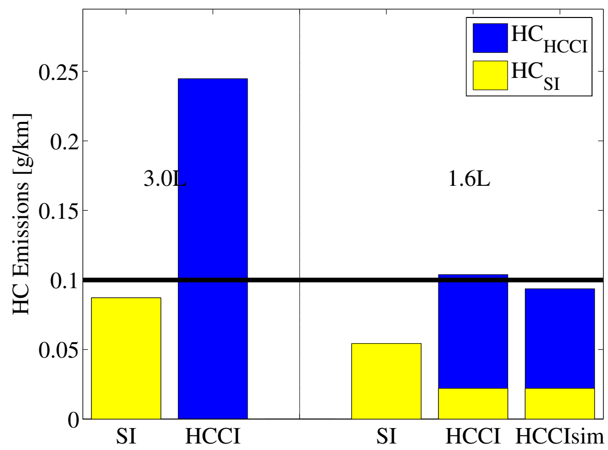

Figure 25 HC emissions after catalyst for all five test cases.

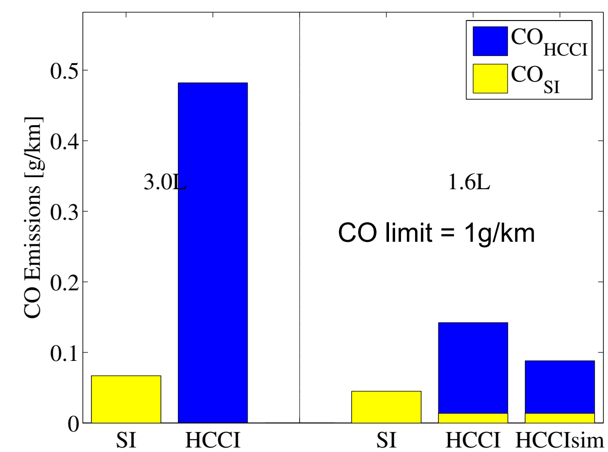

Figure 26 CO emissions after catalyst for all five test cases.

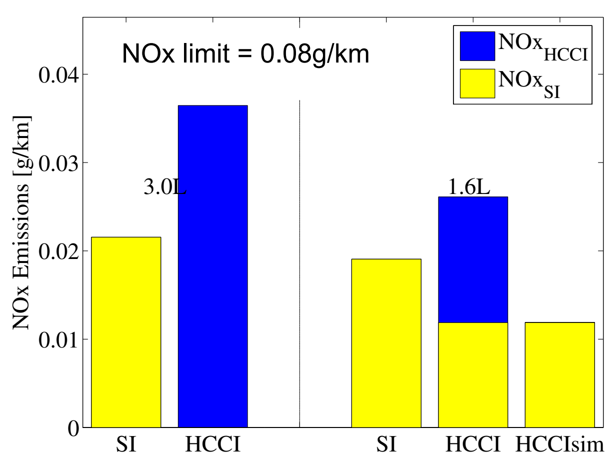

Figure 27 NOx emissions after catalyst for all five test cases.

The CO emissions in Figure 26 are all well below the limit of 1.0 g/km. The same holds for the NOx emissions in Figure 27, which are below the limit of 0.08 g/km. However there is quite a big improvement potential from transient 1.6L HCCI to the HCCIsim. The difference between ideal HCCI and the transient HCCI is that there are no advanced combustion phasings as shown in Figure 15 for the HCCIsim. It might seem strange that the NOx emissions are higher for the 3.0L SI simulation than for the 1.6L SI simulation. This can be explained by the lower load for the scaled 3.0L engine does not produce that much lower NOx emissions to compensate for the scaling effect up to 3.0L compared to the somewhat higher NOx levels at higher load for the 1.6L SI.

DISCUSSION

By running in HCCI 81% of the time a fuel consumption of 6.8L/100km is achieved, which is an improvement of 13% compared to the pure 1.6L SI. As shown in Figure 17 there is a 15% improvement potential when using this particular engine, but the potential of the concept is larger than that. It should be remembered that the SI SVC already has low fuel consumption, shown in Figure 11, and if the HCCI SVC would be compared to another comparable engine the figures would be greater, but there are some major drawbacks with the HCCI SVC that leaves room for improvement of both fuel consumption and emissions.

- High heat losses due to unfavorable volume to area ratio [12]

- High Friction Mean Effective Pressure (FMEP) [17]

The high heat losses result in an even higher demand for CR or inlet air temperature. Since there are limitations on how much energy that can be gained from the exhaust, it is necessary to increase CR even more, which increases heat losses even more. The FMEP of 1.2 bar are due to the rather robust engine design of the downsized SVC engine [26] and, can be compared to the by Fuerhapter et al. [33,34] optimized HCCI engine with a FMEP of approximately 0.9 bar and a fuel consumption reduction of 12.8% during a drive cycle test compared to their SI counterpart.

The HC emissions improvement potential is 9.7%, while the CO and NOx are 38% and 54% respectively. This means that the improvement potential measured in emissions are larger than that of the fuel consumption. This can be explained by the rather flat maximum brake torque curve as a function of CR [16]. When increasing CR above the mapped value, fuel consumption increase very moderately, due to increased heat losses, but the CO emissions increase more, due to excessively fast expansion rate [12]. A solution to decrease CO emissions at low load is to advance CA50, but this is very demanding for the controller, since a fast increase in load demands an almost equally fast retardation of CA50 to avoid excessive rate of pressure rise and NOx emissions. However the cylinder wall temperature acts as a low pass filter, which helps the controller.

89% of all misfires, as defined by the control program's apparent heat release analysis [13], occur at loads below 0 bar BMEP. This means that the most misfires occur when the injected fuel amount is comparably small and hence the so called misfires have small effect on emissions and fuel economy. The total number of misfires above 0 bar BMEP is 407, which is merely 0.5% of the total number of engine cycles during the drive cycle.

Due to the difficulties to identify a model at retarded CA50s [23], the designed controller has to be fairly slow at retarded CA50s or else it will become unstable. This results in a somewhat poor controller at retarded combustion phasings, which results in some total misfires seen in Figure 14 and Figure 15. When there are misfires on one or two cylinders the load controller increases fuel amount to keep the desired load, which leads to a higher load in the other cylinders that sometimes, if load is too high, results in excessive noise and NOx production.

By performing a system identification with less disturbance on the variables at retarded combustion phasing and by running in closed-loop with a slow integrator it is believed that a suitable model for CA50 later than approximately 9 CAD ATDC can be identified, which would improve performance by avoiding misfires and using more ideal CA50 at all times. By enabling more retarded combustion phasing it is possible to increase the maximum load since maximum rate of pressure rise and peak cylinder pressure are strong functions of CA50.

By increasing the load from 3 to 4 bar BMEP, which is the approximate maximum load at mean steady state load points, the total time in HCCI mode can be increased from 81% to 90%. This will give an additional gain in fuel consumption and by calculating from mean steady state load data at 2000 rpm and 4 bar BMEP from the SI SVC and the HCCI SVC a gain of 21% in fuel consumption is achieved for the HCCI operation. The maximum steady state load curve in Figure 10 shows that if using that curve as maximum load limit 4 bar BMEP is reached over a rather large speed range, which would result in the 21% improvement in fuel consumption and if considering the 3% improvement potential for the "ideal" HCCI compared to the transient HCCI a fair gain with the current controller would be 18% compared to the SI SVC engine. It should be noted that the 3% improvement potential in fuel consumption is not entirely due to the slow controller at retarded CA50, but also due to the unfortunate bug in the control program, which makes the throttles oscillate for a couple of engine cycles when changing CLCC controller.

Zhao et al. [35] showed an improvement of 4.7% in fuel economy during a simulated HCCI-SI drive cycle test where HCCI is achieved by trapping hot residuals. The fairly low improvement in fuel economy is mainly due to the limited minimum load range. This limitation is not present in the inlet air preheated HCCI presented here, where higher CRs are used to increase the load range when inlet air temperature is not high enough.

CONCLUSIONS

- The fast thermal management state feedback controller enables combustion phasing control of random input disturbance, i.e. a drive cycle where load and speed are changed randomly seen from the controller's point of view.

- To increase control authority at low engine speeds, the PID based closed-loop combustion control using compression ratio is applied below 1500 rpm, while the fast thermal management is used for slow cylinder balancing. At speeds above 1500 rpm the air flow over the throttles are large enough to get control authority and the state feedback based fast thermal management is used.

- A combination of HCCI and SI operation is superior to the scaled HCCI approach, which suffers from low mechanical efficiency at low load when running the Saab variable compression engine in the EC2000 drive cycle, according to directive 98/69/EC of the European Parliament.

- By combining real transient HCCI data from the drive cycle test with interpolated mean steady state SI data a mean fuel consumption of 6.8L/100km is reached. An improvement of 13% compared to the low fuel consumption optimized Saab variable compression SI engine and if increasing HCCI load to 4 bar BMEP an approximate improvement of 18% is possible.

- The need of control authority, i.e. to avoid saturation of the fast thermal management throttles, results in increased compression ratio compared to previous steady state tests. This results in an increase of CO emissions.

- Both CO and NOx emissions are well below the Euro IV limits, while the HC emissions are slightly above the limit when calculated without cold start.

- If looking at fuel consumption the current PID and state feedback controllers are good enough, but the emissions could be decreased even more with improved controllers, especially with a state feedback controller, which handles retarded combustion phasings better.

REFERENCES

1. S: Onishi, S. Hong Jo, K. Shoda, P Do Jo, S. Kato, ”Active Thermo-Atmosphere Combustion (ATAC) – A New Combustion Process for Internal Combustion Engines”, SAE790501
2. Y. Ishibashi, M. Asai, ”Improving the Exhaust Emissions of Two-Stroke Engines by Applying the Activated Radical Combustion”, SAE960742
3. P. Najt, D. E. Foster, ”Compression-Ignited Homogeneous Charge Combustion”, SAE830264
4. R. H. Thring, ”Homogeneous-Charge Compression-Ignition (HCCI) Engines”, SAE892068
5. M. Stockinger, H. Schäpertöns, P. Kuhlmann, “Versuche an einem gemischansaugenden mit Selbszündung”, MTZ 53 (1992).
6. M. Christensen, P. Einewall, B. Johansson, ”Homogeneous Charge Compression Ignition (HCCI) Using Isooctane, Ethanol and Natural Gas – A Comparison to Spark Ignition Operation", SAE972874
7. M. Christensen, B. Johansson, P. Amnéus, F. Mauss, ”Supercharged Homogeneous Charge Compression Ignition”, SAE 980787
8. M. Christensen, B. Johansson: ”Influence of Mixture Quality on Homogeneous Charge Compression Ignition”, SAE982454
9. M. Christensen, B. Johansson, ”Homogeneous Charge Compression Ignition with Water Injection”, SAE1999-01-0182
10. J. Li, H. Zhao, N. Ladommatos, T. Ma, “Research and development of controlled auto-ignition (CAI) combustion in a 4-stroke multi cylinder gasoline engine”, SAE-2001-01-3608
11. G. M. Shaver, J. C. Gerdes, M. Roelle, “Physics-Based Closed-Loop Control of Phasing, Peak Pressure and Work Output in HCCI Engines Utilizing Variable Valve Actuation” ACC 467, 2004
12. G. Haraldsson, J. Hyvönen, P. Tunestål, B. Johansson, ”HCCI Combustion Phasing in a Multi Cylinder Engine Using Variable Compression Ratio”, SAE 2002-01-2858.
13. J-O. Olsson, P. Tunestål, B. Johansson, “Closed-Loop Control of an HCCI Engine”, SAE 2001-01-1031
14. M. Christensen, A. Hultqvist, B. Johansson, “Demonstrating the Multi Fuel Capability for a Homogeneous Charge Compression ignition Engine with Variable Compression Ratio”, SAE 1999-01-3679
15. J-O. Olsson, P. Tunestål, B. Johansson, S. Fiveland, R. Agama, M. Willi, D. Assanis, “Compression Ratio Influence on Maximum Load of a Natural Gas Fueled HCCI Engine” SAE 2002-01-0111
16. J. Hyvönen, G. Haraldsson, B. Johansson, ”Operating range in a Multi Cylinder engine using Variable Compression Ratio” JSAE 20030178/ SAE 2003-01-182
17. J. Hyvönen, G. Haraldsson, B. Johansson, “Supercharging HCCI to extend the operating range in a Multi-Cylinder VCR-HCCI engine” SAE 2003-01-3214
18. G. Haraldsson, J. Hyvönen, P. Tunestål, B. Johansson, ”HCCI Combustion Phasing with Closed-Loop Combustion Control Using Variable Compression Ratio in a Multi Cylinder Engine”, JSAE 200301126/SAE 2003-01-1830
19. F. Agrell, H-E. Ångström, B. Eriksson, J. Wikander, J. Linderyd, “Integrated Simulation and Engine Test of Closed Loop HCCI Control by Aid of Variable Valve Timings”, SAE 2003-01-0748
20. J. Yang, T. Culp, T. Kenney, “Development of a Gasoline Engine System Using HCCI Technology – The Concept and the Test Results” SAE 2002-01-2832
21. G. Haraldsson, J. Hyvönen, P. Tunestål, B. Johansson, ”HCCI Closed-Loop Combustion Control Using Fast Thermal Management”, SAE 2004-01-0943
22. J. Hyvönen, G. Haraldsson, B. Johansson, ” Balancing cylinder-to-cylinder variations in a Multi-Cylinder VCR-HCCI engine”, SAE 2004-01-1897
23. R. Pfeiffer, G. Haraldsson, J-O. Olsson, P. Tunestål, R. Johansson, B. Johansson, “System identification and LQG control of Variable-Compression HCCI Engine Dynamics”, CCA/ISIC/CACSD Conference in Taiwan 2004
24. J. Hyvönen, G. Haraldsson, B. Johansson, “Operating conditions using spark assisted HCCI combustion during combustion mode transfer to SI in a Multi-Cylinder VCR-HCCI engine” SAE 2005-01-0109
25. Directive 98/69/EC of the European Parliament and of the Council of 13 October 1998
26. H. Drangel, L. Bergsten, ”The new Saab SVC Engine - An Interaction of Variable Compression Ratio, High Pressure Supercharging and Downsizing for Considerably Reduced Fuel Consumption”, 9. Aachener Kolloquium Fahrzeug- und Motorentechnik 2000
27. L. Ljung, “System Identification, Theory for the user”, Prentice Hall 1999
28. T. Glad, L. Ljung, “Reglerteknik Grundläggande Teori”, ISBN 91-44-17892-1, 1997
29. J. Bengtsson, “Closed-Loop Control of HCCI Engine Dynamics” Doctoral Thesis, ISSN 0280 5316, ISRN LUTFD2/TFRT—1070—SE, Department of Automatic Control, Lund Institute of Technology/Lund University, 2004
30. G. Spencer, ” Capitol Comment 266 - The ACEA Agreement: Reopening the Kyoto Café”,

http://www.cse.org/informed/issues_template.php?issue_id=435, 2004
31. N. A. Henein, M. K. Tagomori, M. K. Yassine, T. W. Asmus, C. P. Thomas, P. G. Hartman, ”Cycle-by Cycle Analysis of HC Emissions During Cold Start of Gasoline Engines”, SAE 952402
32. T. H. Ballinger, P. J. Andersen, ”Vehicle Comparison of Advanced Three-Way Catalysts and Hydrocarbon Trap Catalysts”, SAE-2002-01.0730
33. A. Fuerhapter, E. Unger, W. F. Piock, G. K. Fraidl, “The new AVL CSI Engine – HCCI Operation on a Multi Cylinder Engine”, SAE-2004-01-0551
34. A. Fuerhapter, W. F. Piock, G. K. Fraidl, “The AVL CSI Engine with Controlled Autoignition an Application Example of HCCI”, SAE HCCI Symposium, Berkeley, 2004
35. H. Zhao, J. Li, T. Ma, N. Ladommatos, Performance and Analysis of a 4-Stroke Multi-Cylinder Gasoline Engine with CAI Combustion”, SAE-2002-01-0420

CONTACT

Göran Haraldsson, MSc M. E.
E-mail: goran.haraldsson@vok.lth.se

Jari Hyvönen, MSc M. E.
E-mail: jari.hyvonen@vok.lth.se

Per Tunestål, Assistant Professor
E-mail: per.tunestal@vok.lth.se

Bengt Johansson, Professor.
E-mail: bengt.johansson@vok.lth.se

Department of Heat and Power Engineering, Division of Combustion Engines, Lund Institute of Technology, P.O. Box 118, SE-221 00 Lund, Sweden.

DEFINITIONS, ACRONYMS, ABBREVIATIONS

A/D: Analogue to Digital

ATDC: After Top Dead Centre

BSFC: Brake Specific Fuel Consumption

BMEP: Brake Mean Effective Pressure

BTDC: Before Top Dead Centre

CAD: Crank Angle Degree

CA50: Crank Angle for 50% burned

CI: Compression Ignition

CLCC: Closed-Loop Combustion Control

CR: Compression Ratio

DC: Direct Current

EC2000: Drive cycle also (Urban+extra urban, Rev. ECE+EUDC, NEDC.

EGR: Exhaust Gas Recirculation

FH: Fuel Heat

FMEP: Friction Mean Effective Pressure

FTM: Fast Thermal Management

HCCI: Homogeneous Charge Compression Ignition

LQG: Linear Quadratic Gaussian

LTR: Low Temperature Reactions

MON: Motored Octane Number

PCI: Peripheral Interface Controller

PID: Proportional Integral Derivative

PRBS: Pseudo Random Binary Sequences

PWM: Pulse Width Modulation

RON: Research Octane Number

SI: Spark Ignition

SVC: Saab Variable Compression

TDC: Top Dead Center

TWC: Three Way Catalyst

VCR: Variable Compression Ratio